

## REINFORCING STRUCTURES IN AVIAN WING BONES

E. Novitskaya<sup>1\*</sup>, M.S. Ribero Vairo<sup>1,2</sup>, J. Kiang<sup>1</sup>, M.A. Meyers<sup>1</sup>, J. McKittrick<sup>1</sup>

<sup>1</sup>University of California, San Diego, Department of Mechanical and Aerospace Engineering and Materials Science and Engineering Program, 9500 Gilman Dr., La Jolla, CA 92093, USA

<sup>2</sup>Universidad Nacional de Cuyo, Centro Universitario, Facultad de Ingenieria and ITIC, M5502JMA, Mendoza, Argentina

### ABSTRACT

Nearly all species of modern birds are capable of flight; therefore mechanical competency of appendages and the rigidity of their skeletal system should be optimized. Birds have developed extremely lightweight skeletal systems that help aid in the generation of lift and thrust forces as well as helping them maintain flight over, in many cases, extended periods of time. The humerus and ulna of different species of birds (flapping, flapping/soaring, flapping/gliding, and non-flying) have been analyzed by optical microscopy and mechanical testing. The reinforcing structures found within bones vary from species to species, depending on how a particular species utilizes its wings. Interestingly, reinforcing ridges and struts have been found within certain sections of the bones of flapping/soaring and flapping/gliding birds (vulture and sea gull), while the bones from the flapping bird (raven) and non-flying bird (domestic duck) did not have supporting structures of any kind. The presence of these reinforcing structures increases the resistance to torsion and flexure with a minimum weight penalty, and is therefore of importance in flapping/gliding birds. Vickers hardness testing was performed on the compact section of the bones of all bird species. The data from the mechanical testing were compared with microstructural observations to determine the relevance behind the reinforcing structures and its mechanical and biological role. Finite element analysis was used to model the mechanical response of vulture ulna in torsion.

### 1. INTRODUCTION

Mechanical engineering is an interdisciplinary field that encompasses studies such as solid mechanics and material science. By understanding and using the core concepts behind these studies, mechanical engineers are able to analyze, design, manufacture, and maintain mechanical systems. Biomimetics is the application of the structure and function of biological systems for the design of new machines and materials, and is emerging as a new area of interest that opens up a completely different view on mechanical engineering.

In nature, excellent examples of engineering solutions are found. These engineering solutions have been perfected over millions of years of evolution. By studying and understanding lessons from nature, new or better designs of materials and structures can be made<sup>1</sup>. For biomimetics, it is important to have a clear understanding of biology.

Outstanding examples of structural adaptation are avian wing bones. This has been recognized close to one hundred years ago by Darcy Thompson<sup>2</sup>. These bones have evolved over time to allow the birds to achieve and maintain flight. One adaptation is the fusion of several bones into a single ossification. The carpometacarpus (blade-like structure of wrist and hand bones) is an example of fused bird bones, which helps to provide additional strength to the wing<sup>3,4</sup>. By fusing the bones, the total number of bones found within a bird skeletal system is far less than that of other terrestrial vertebrates<sup>3,4</sup>. Additionally, the skeleton becomes much more lightweight as well as rigid. Another adaptation for flight is that many of the bones are hollow or semi-hollow. The hollow bones help to

---

\* Corresponding author, phone: 858-534-5513, fax: 858-534-5698, e-mail: eevdokim@ucsd.edu

## Reinforcing Structures in Avian Wing Bones

offset the high-energy cost of flight<sup>4</sup>. In addition, air pockets (pneumatic foramina<sup>3</sup>) often form within the hollow or semi-hollow bones of birds (e.g., humerus and skull). These pockets are part of the “flow-through ventilation” system that avian species use to move air through their lungs, forming pneumatic bones<sup>5,6</sup>.

The bird wing consists of several main bones such as humerus (‘upper arm’), radius and ulna (‘forearm’), carpometacarpus to form the ‘wrist’ and ‘hand’ of the bird, and the digits (‘fingers’) that are fused together. The main flight muscles of the breast are attached only to a humerus bone; therefore this bone has an important role of bearing the large forces during the flight<sup>4</sup>. The ulna is one of two bones that support the midsection of the wing. For the flying birds the humerus is usually shorter and thicker compare to ulna, since it needs to withstand larger forces during the flight<sup>4</sup>. In addition, the bones of various avian species have microstructural features (osteonal structure, Haversian canals, and lacunae) similar to other mammalian long bones<sup>6</sup>.

Some birds achieve and maintain flight by flapping their wings as well as soaring through the air (flapping/soaring birds<sup>8</sup>, e.g. vultures, eagles); others are flapping and gliding (flapping/gliding birds<sup>8</sup>, e.g. sea gulls, pelicans). Furthermore, some birds are able to alternate between flapping their wings with only periodic gliding (flapping birds, e.g. ravens, crows). Some birds are flightless due to environmental and habitat conditions of their growth (e.g. domestic ducks, emus).

It has been shown that reinforcing structures are found within wing bones in the places of maximum torsional and bending moments<sup>4,9</sup>. These structures (struts) mostly appear at the places “in need”, preventing the buckling of bone walls due to internal loads<sup>9</sup>. Another type of supporting structure (ridges) was found inside the wing bones of flapping/soaring and flapping/gliding birds<sup>8</sup>. These structures are similar to ship supporting trusses which have a function of optimization and redistributing of external stresses. A detailed analysis of reinforcing structures (both struts and ridges), and mechanical properties of two wing bones, the humerus and ulna, from flapping, flapping/soaring, flapping/gliding, as well as a non-flying bird was performed in this study. Additionally, a first approach on the understanding of the mechanical behavior of bird wing bones in torsion using finite element analysis (FEA) is presented in this work.

## 2. MATERIALS AND METHODS

### 2.1 Sample preparation

Bone samples from ulna and humerus were gathered from a flapping/soaring bird (the Turkey Vulture, *Cathartes aura*), a flapping/gliding bird (the California Gull, *Larus californicus*), a flapping bird (the Common Raven, *Corvus corax*) and a non-flying bird (the Pekin Duck, *Anas peking*). Bones were stored in ambient dry condition at room temperature and normal humidity.

### 2.2 Mineral content

The mineral content of bird bones was measured by weight. First, cleaned samples (about 1 cm height cylinders) were submerged in Hank's balance saline solution for 24 hr for rehydration. Then, the water content was evaporated by heating the bones in an oven at 105°C for four hours. The weights of the individual samples were measured before and after the heating processes, providing the information about water content of the bones. Next, bone samples were further heated in an oven for 24 hours at 550°C to eliminate the proteins. The weights of the individual samples were measured before and after the heating process. Weight percent of minerals (wt.%) was calculated by dividing the weight after by the weight before heating.

### 2.3 Structural characterization

Cross-sections of ulnae and humeri were prepared for each bird species; next they were embedded into epoxy and polished for future optical observation and hardness testing. Samples from

all four species were analyzed by optical microscopy using Zeiss Axio imager equipped with CCD camera (Zeiss Microimaging Inc., Thornwood, NY), and Keyence VHX1000 microscope (KEYENCE America, Elmwood Park, NJ).

#### 2.4 Image processing

An image processor, ImageJ, was used to analyze the porosity of the bone samples, similar to the porosity analysis by Manilay et al.<sup>10</sup> The Haversian system (including vascular channels and Volkmann's canals), and lacuna spaces were the pore types used for the porosity calculations. Porosity values were calculated dividing the sum of the areas of the pores by the total area of the image.

#### 2.5 Micro-computed tomography ( $\mu$ CT)

A section from a distal part of Turkey Vulture ulna was scanned on a micro-computed tomography ( $\mu$ CT) scanner, Skyscan 1076 (Kontich, Belgium). Bone was scanned inside a dry plastic tube. Imaging was performed at 36  $\mu$ m isotropic voxel sizes applying an electric potential of 70 kV and a current of 200  $\mu$ A, using a 0.5 mm aluminum filter. Images and 3-dimensional (3D) rendered models were developed using Skyscan's DataViewer and CTVox software.

#### 2.6 Hardness testing

Hardness from all four species was measured using a LECO M-400-H1 hardness testing machine equipped with a Vickers hardness indenter. The cross-sectional bone samples embedded into epoxy were analyzed at different locations to determine the overall hardness distribution across a single cross-section of the bone. Hardness values were averaged from 20 micro-indentations. A load of 10 g<sub>F</sub> was used to indent the exposed surfaces.

#### 2.7 Statistical analysis

One-way ANOVA analysis was performed to determine significant differences between the hardness data for humerus and ulna of the same bird species, and among species. The criterion for statistical significance was  $p < 0.05$ .

#### 2.8 Finite element analysis (FEA)

A small section of the vulture ulna (a cylinder with 13 mm in height, 9 mm in diameter, and 0.8 mm in wall thickness) from the distal end (Figures 1, 2) was analyzed in torsion by finite element program LS-DYNA (Version 971)<sup>11</sup>. The geometry was obtained from  $\mu$ -CT images, and discretized with 151,083 tetrahedral solid elements with aspect ratios between 1.03 and 5.96. A linear elastic isotropic model with a homogeneous distribution of properties was considered. The elastic properties were taken from the literature<sup>9</sup> and from mechanical testing assuming isotropy as: Young's modulus  $E = 20$  GPa, Poisson's ratio ( $\nu$ ) = 0.3. The geometry discretization and boundary conditions are shown in Figure 1. Nodes in the bottom of the samples were constrained to a zero displacement, while the top ones were subjected to an angular velocity of 0.04 rad s<sup>-1</sup>, with a final rotation of 0.2 rad to avoid geometrical nonlinearities during the simulation. The rotational axis was coincident with the torque vector  $T$  (Figure 1b), and applied along the center of inertia of the whole sample. No inertia effects were considered in the simulation. The final result was shown as a von Mises stress distribution.

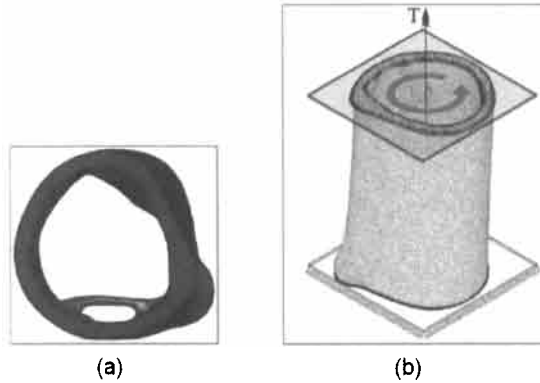


Figure 1. (a) The  $\mu$ CT image of the section of the Turkey Vulture ulna (top view). (b) Geometry discretization and boundary conditions for the section. The planes on the top and bottom of the sample are defined by the end nodes.

### 3. RESULTS AND DISCUSSION

The left wing of the Turkey Vulture is shown in Figure 2 as an example of the overall bone configuration of a bird wing.

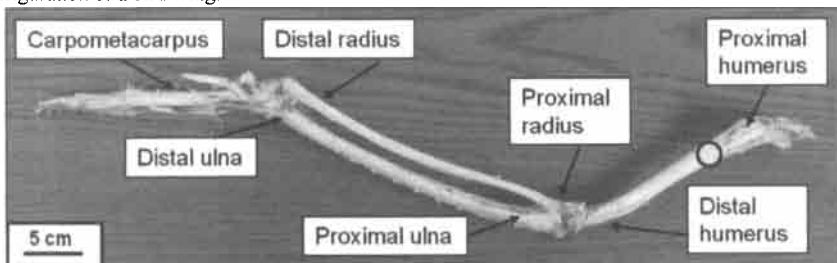


Figure 2. Left wing of the Turkey Vulture. Proximal and distal ends of humerus, ulna, and radius are marked. The yellow dot shows the point of maximum bending and torsional moments carried by the humerus in flight<sup>9</sup>.

Proximal (closest to body) and distal (farthest from body) ends of humerus, ulna, and radius are marked. The yellow dot shows the point of maximum bending and torsional moments carried by the humerus in flight<sup>9</sup>. A basic comparison of the sizes of ulnae and humeri for flying (vulture) and non-flying (duck) birds are shown in Figure 3. The proximal and distal ends of the bones are shown. It is clear that for flying birds ulna is longer compare to humerus, while it is opposite for non-flying birds<sup>4,9</sup>. The ratio between the lengths of humeri and ulnae was similar for the flying birds (0.8-0.9), while it was  $\sim 1.5$  for the non-flying bird. The ways birds use their wings, as well as torsional and flexure stresses that bones experience during the flight for the former case and lack of these events for the latter one are the main reasons for this fact.

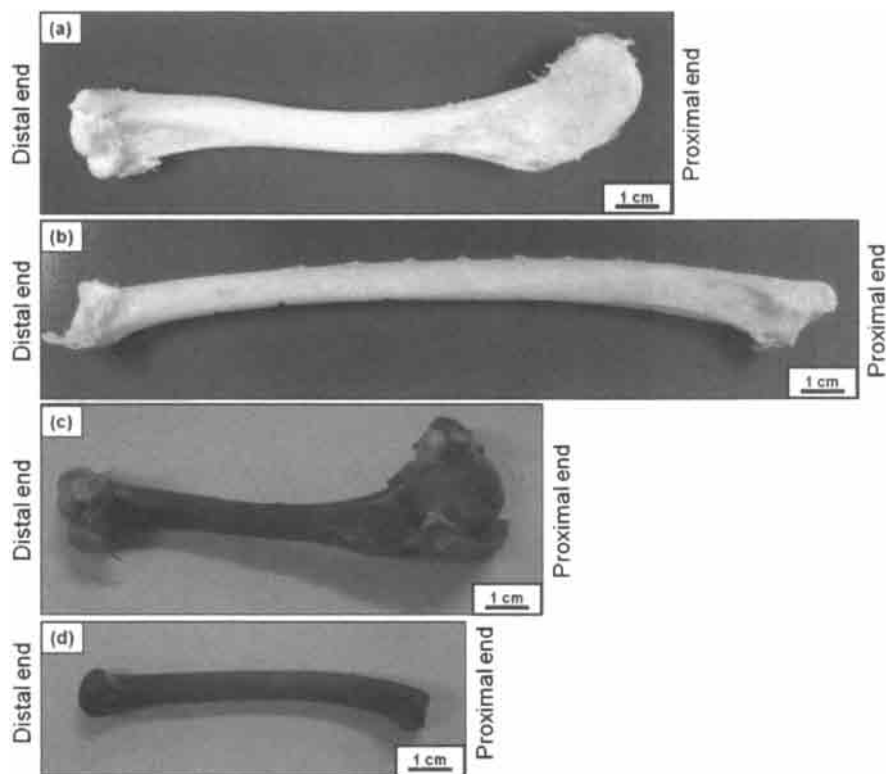


Figure 3. Humerus (a) and ulna (b) of the Turkey Vulture, and humerus (c) and ulna (d) of the Pekin Duck.

Microstructural analysis was performed on the entire cross-sections of ulnae and humeri for all species; representative images of ulnae cross-sections are shown in Figure 4. It is clear that thickness of the bone wall is not uniform for all flying birds due to presence of external pressure and stress distribution on them during the flight. Additionally, bones from flapping/soaring and flapping/gliding birds have ovalized cross-sections, while bones from flapping and non-flying birds have more circular cross-sections. The ulna from non-flying bird (duck) has the most circular cross-section. Furthermore, ulnae of the vulture and the gull have the reinforcing structures (struts), while ulnae of the raven and the duck lack them (Figure 4). These struts are thought to be in the places “in need” to support the bone against extensive ovalization during torsional and flexure loading<sup>9</sup>. The ovalization usually appears in bones that are subjected to high bending moments during flight. The ovalization changes the cross-sectional shape and weakens the whole bone structure resulting in unstable elastic deformation<sup>9</sup>. This weakening can be corrected by the presence of relatively long struts that oriented at 45° to the bone wall.

One should distinguish the two types of reinforcing struts; the first one supports the hollow center of the bone against the ovalization, and the second one (an array of crisscrossing struts, with the appearance of a truss) appears at places “in need” supporting the bone against the extensive

## Reinforcing Structures in Avian Wing Bones

torsional stresses during the flight (Figure 5a)<sup>8</sup>. Another type of reinforcing structure that helps to withstand the excessive torsional moments of flight are reinforcing ridges (Figure 5b)<sup>9</sup>.

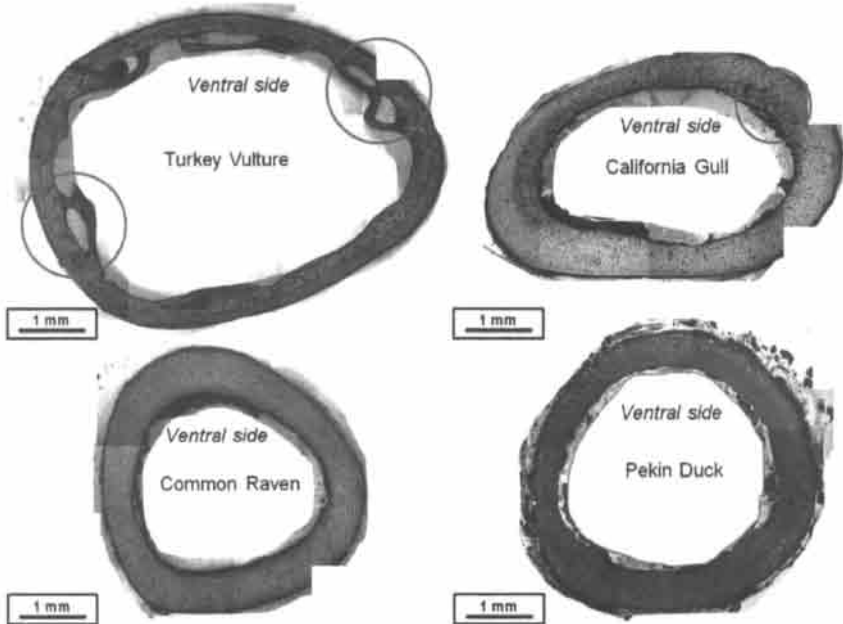


Figure 4. Optical microscopic images of the cross-sections of the ulnae. Struts are shown in red circles.

More detailed analysis of humeri verified that the truss structure is mainly located at the point of pectoral muscle attachment, approximately one-third from the proximal end of humerus at the point of maximum bending and torsional moments carried by the bone in flight<sup>9</sup>, as shown in Figure 2. In addition, the struts and ridges were mainly found on ventral side of the humeri and ulnae (Figure 4). Furthermore, the non-flying bird (duck) does not have reinforcing structures; instead both the ulna and humerus have trabecular bone at both proximal and distal ends, similar to mammalian long bones.

Figure 6 shows representative optical images of microstructure of the humeri for all species. The microstructures of the vulture, gull, and raven are similar to fully mature mammalian bone, due to the presence of well-developed microstructural features, such as osteons, Haversian systems, and lacunae, which are observed in the images. The duck humerus is extremely porous and has a less organized structure due to relatively young age of this bird (6 month old) compared to all other bird species (several years old). Reinforcing structures were found in humeri of the flapping/soaring and flapping/gliding birds (Figure 6a and 6b), while humeri of flapping and non-flying birds did not have those structures (Figure 6c and 6d). This observation indicates that reinforcing structures are at the places "in need" that subjected to the maximum stresses during the bird flight.

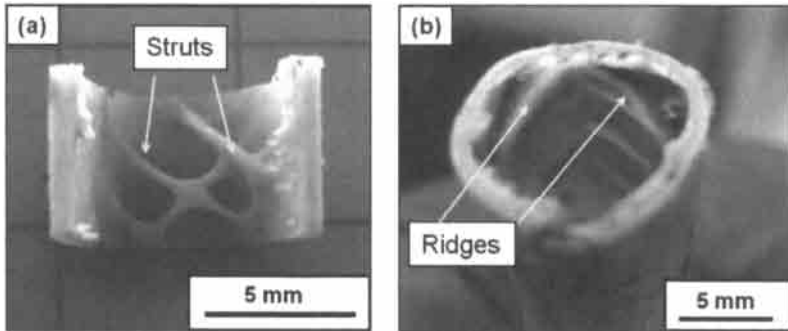


Figure 5. Optical image of (a) reinforcing an array of struts (truss), and (b) reinforcing ridges inside the Turkey Vulture ulna.

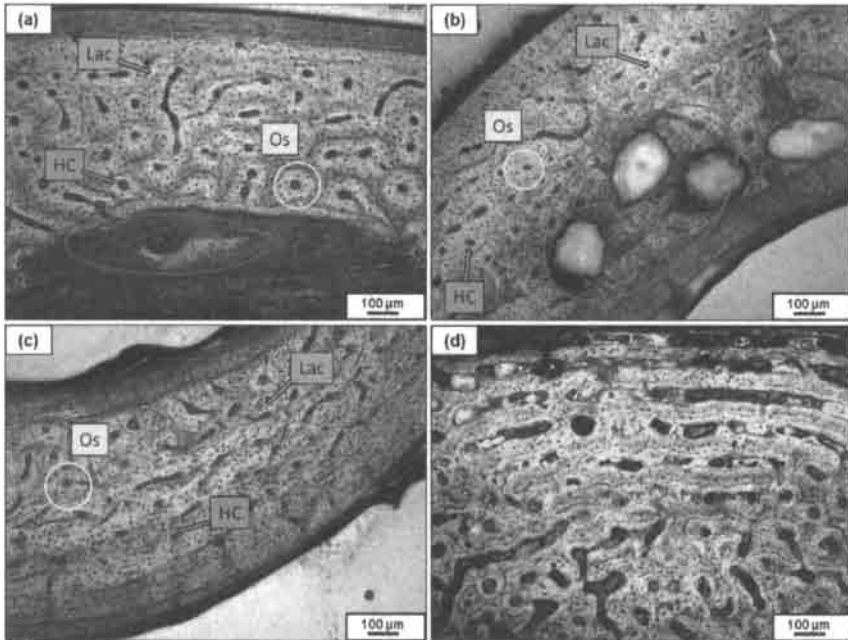


Figure 6. Optical images of humeri of the (a) Turkey Vulture, (b) California Gull, (c) Common Raven and (d) Pekin Duck, showing microstructural features: osteons (Os), lacunae (Lac), and Haversian channels (HC). Ridges are shown in large red ovals.

The data for mineral content, density, and porosity of humeri and ulnae are summarized in Table I. The amount of porosity and mineral content were mostly dependent on the bone maturity level, rather than on the taxa (values for porosity and mineral content were very similar for ulna and

humerus of the same species). The amount of porosity for mature birds was found to be between 9-14%. Young duck bones have the highest amount of porosity (~20%) in agreement with our previous study finding young bovine bone to have more porosity than the mature ones<sup>10</sup>. Duck bones also have the lowest mineral content. The density of the humerus was found to be slightly higher than the ulna for flapping/soaring and flapping/gliding birds (vulture and gull), while opposite was found for the flapping and non-flying ones (raven and duck). A possible explanation is that typically gliding and soaring birds have a longer wingspan, resulting in a long moment arm both for torsional and bending moment decomposition of the lift force<sup>9</sup>, which translates into a higher stress in the humerus, therefore its density is slightly higher compared to that of ulna. Table I also compared the bird bones with bovine skeletal bone. The bird bones have a smaller amount of minerals and a much larger amount of porosity, which in combination yields a lower density, an advantage for flight.

Table I. Mineral content, density and porosity for humerus and ulna bones of four bird species.

	Mineral content (wt.%)		Density (gm/cm <sup>3</sup> )		Porosity (%)	
	Humerus	Ulna	Humerus	Ulna	Humerus	Ulna
Turkey Vulture	60 ± 1	61 ± 2	1.6±0.1	1.2±0.1	11±2	11±2
California Gull	66 ± 1	65 ± 2	1.4±0.1	1.3±0.1	13±3	9±1
Common Raven	64±2	63±1	1.3±0.1	1.5±0.1	14±1	13±3
Pekin Duck	43±1	43±1	1.2±0.2	1.3±0.2	20±4	20±4
Bovine cortical femur bone <sup>14</sup>	65 ± 2		2.0 ± 0.2		8 ± 1	

The Vickers hardness results are summarized in Figure 7. Porosity is one of the main factors contributing to the mechanical properties of bone, along with taxa, hydration condition, anatomical direction, and load distribution<sup>8,13</sup>. Since porosity has adverse effect on strength, the highest porosity of the younger duck bones is in agreement with the smallest hardness values, demonstrating that the mature bone is stronger than the young one. Furthermore, the humerus was found to be significantly harder ( $p < 0.05$ ) than the ulna for the gull (flapping/gliding bird), while it was opposite for the raven (flapping bird). Potential differences in age (and as a result, diverse microstructure and amount of porosity), as well as different flight behavior (flapping/gliding versus flapping) of these birds are the possible reasons for these results. The hardness values for humerus and ulna were almost the same for the vulture and the duck. These findings again demonstrate that structure and mechanical properties of bird wing bones are optimized for the stresses that those bones are subjected to during bird life. In comparison, the hardness for bovine femur cortical bone is in the range of 550-700 MPa.

To assess the stress distribution in a wing bones subjected to torsion, FEA was applied to the small cylindrical section of the Turkey Vulture ulna (Figure 1b). Two struts with a circular cross-section and diameter equal to the half of the cylinder wall thickness were found in that sample (Figure 1a). The maximum effective strain for the final state of deformation reached a value of 0.13, and no geometrical nonlinearities were developed during the simulation. The von Mises stress distribution obtained by FEA on the top of the bone is shown in Figure 8a, and on the internal bone walls in Figure 8b and 8c. For the given direction of rotation (Figure 1b), the minimum values of von Mises stress were found in the struts and at the immediate areas of their attachment to the bone walls (those areas can be interpreted as a thickening of the cylinder walls). Quantitatively, the struts are subjected to stresses on the order of 15% of those of the inner walls. Due to a larger surface of attachment of the strut in Figure 8c compared to the strut in Figure 8b, the influence of the former one is more notable. These are the preliminary results, and a more detailed modeling of torsional and bending properties for different bird wing bones is being conducted.

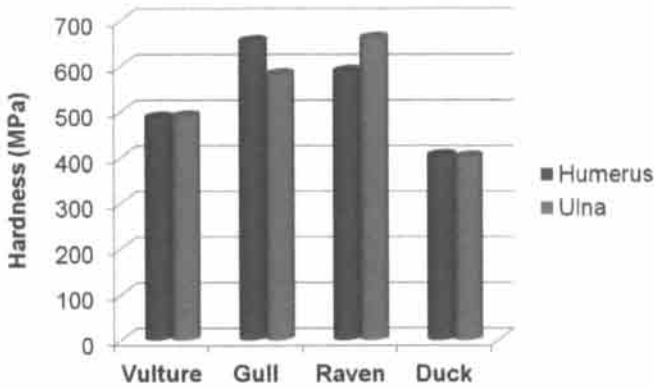


Figure 7. Vickers hardness data for humerus and ulna for different bird species.

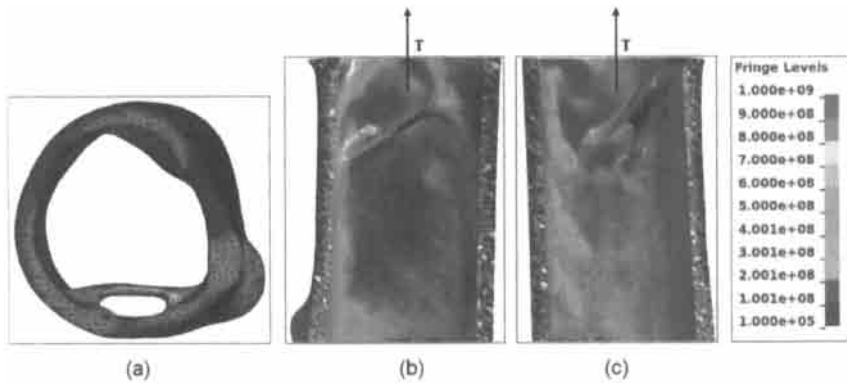


Figure 8. The final von Mises stress distribution [Pa] for the Turkey Vulture ulna section under torsion. (a) Top view, (b) and (c) interiors of two halves.

#### 4. CONCLUSIONS

The structure and mechanical properties of bird humeri and ulnae from flapping/soaring (the Turkey Vulture, *Cathartes aura*), flapping/gliding (the California Gull, *Larus californicus*), flapping (the Common Raven, *Corvus corax*), and non-flying (the Pekin Duck, *Anas peking*) birds, were investigated by optical microscopy and Vickers hardness testing. The torsional mechanical behavior of a section of the Turkey Vulture ulna was simulated using FEA. The main findings are:

- Wing bones from non-flying birds were found to have a circular cross-section, as well as a uniform thickness around the cross-section due to lack of torsional and bending stresses. In contrast, wing bones from the flying birds experience ovalization and non-uniformity of thickness around the cross-sections due to the large torsional and bending moments during the flight;

## Reinforcing Structures in Avian Wing Bones

- Flying birds have reinforcing structures (struts and ridges) inside their wing bones to optimize and redistribute bending and torsion stresses during the flight;
- Reinforcing struts are roughly at 45° to the bone walls to evenly support the whole structure;
- The humerus was found to be slightly denser compared to ulna for flapping/soaring and flapping/gliding birds, to provide better support for a bird body and redistribute stresses during the flight;
- The detailed geometry measurements by  $\mu$ CT scan together with the capabilities of FEA allowed for an adequate stress distribution determination;
- In the simulation of torsion, the struts and the area around them show the lowest values of von Mises stress on the inner surface of bone under a torsional stress.

### ACKNOWLEDGEMENTS

We thank Esther Cory and Professor Robert Sah (UCSD) for the help with  $\mu$ CT imaging, Drs. Cesar Flores and Juan Hermida (Shiley Center for Orthopaedic Research & Education) for their assistance in the a mesh preparation for the FEA, Professor Colin Pennycuick (University of Bristol) and Carlos Ruestes (UCSD) for their valuable insights and discussions. This research was funded by the National Science Foundation, Division of Materials Research, Ceramics Program (DMR 1006931).

### REFERENCES

- <sup>1</sup>P.-Y. Chen, J. McKittrick, M.A. Meyers, Biological materials: Functional adaptations and bioinspired designs, *Prog. Mater. Sci.*, **57**, 1492-704, (2012).
- <sup>2</sup>D.W. Thompson, *On Growth and Form*, 2<sup>nd</sup> Ed. Cambridge University Press, Cambridge, UK, 460, (1968).
- <sup>3</sup>A. Wolfson, *Recent Studies in Avian Biology*, University of Illinois Press, Urbana (1955).
- <sup>4</sup>N.S. Proctor, P.J. Lynch, *Manual of Ornithology: Avian Structure and Function*, Yale University Press, New Haven, USA, (1993).
- <sup>5</sup>P.M. O'Connor, L.P.A.M. Claessens, Basic avian pulmonary design and flow-through ventilation in non-avian theropod dinosaurs, *Nature*, **436**, 253-256, (2005).
- <sup>6</sup>F.L. Powell, Respiration, in *Sturkie's Avian Physiology*, edited by Whittow GC, Academic Press, San Diego, 233-264, (2000).
- <sup>7</sup>J.D. Currey, *Bones: Structure and Mechanics*, Princeton University Press, Princeton, NJ, (2002).
- <sup>8</sup>B. Bruderer, P. Dieter, A. Boldt, F. Liechti, Wing-beat characteristics of birds recorded with tracking radar and cine camera, *Ibis*, **152**, 272-291, (2010).
- <sup>9</sup>C.J. Pennycuick, *Modeling the Flying Bird*, Elsevier, Oxford, UK, (2007).
- <sup>10</sup>Z. Manilay, E.E. Novitskaya, E. Sadovnikov, J. McKittrick, A comparative study of young and mature bovine cortical bone, *Acta Biomater.*, **9**, 5280-5288, (2013).
- <sup>11</sup>LS-DYNA Theory manual, (2006).
- <sup>12</sup>D. Taylor, J.-H. Dirks, Shape optimization in exoskeletons and endoskeletons: A biomechanics analysis, *J. R. Soc. Interface*, **9**, 3480-3489, (2012).
- <sup>13</sup>E. Novitskaya, P.-Y.Chen, E. Hamed, J. Li, V.A. Lubarda, I. Jasiuk, J. McKittrick, Recent advances on the measurement and calculation of the elastic moduli of cortical and trabecular bone: A review, *Theor. Appl. Mech.*, **38**, 209-297, (2011).
- <sup>14</sup>E. Novitskaya, A.B. Castro-Ceseña, P.-Y. Chen, S. Lee, G. Hirata, V.A. Lubarda, J. McKittrick, Anisotropy in the compressive mechanical properties of bovine cortical bone: Mineral and protein constituents compared with untreated bone, *Acta Biomater.*, **7**, 3170-3177, (2011).